

1974

Heat Transfer Across Carbon-Liquid Helium I Interface

Constantine Antonopoulos
Portland State University

Let us know how access to this document benefits you.

Follow this and additional works at: http://pdxscholar.library.pdx.edu/open_access_etds

 Part of the [Physics Commons](#)

Recommended Citation

Antonopoulos, Constantine, "Heat Transfer Across Carbon-Liquid Helium I Interface" (1974). *Dissertations and Theses*. Paper 2136.

10.15760/etd.2133

This Thesis is brought to you for free and open access. It has been accepted for inclusion in Dissertations and Theses by an authorized administrator of PDXScholar. For more information, please contact pdxscholar@pdx.edu.

AN ABSTRACT OF THE THESIS OF Constantine Antonopoulos
for the Master of Science in Physics presented May 15, 1974.

Title: Heat Transfer Across Carbon - Liquid Helium I
Interface.

APPROVED BY MEMBERS OF THE THESIS COMMITTEE:

[REDACTED]

Laird C. Brodie, Chairman

[REDACTED]

David W. McClure

[REDACTED]

Cecil E. Sanford

[REDACTED]

Jack Semura

Carbon samples were electrically heated while immersed in liquid helium I. Their temperature rise was observed on an oscilloscope as a function of the time after the onset of the electric current. There was no indication of the temperature overshoot previously reported for the case of bismuth in liquid helium.

Reasons are presented for the difference in behavior of carbon and bismuth.

HEAT TRANSFER ACROSS CARBON -
LIQUID HELIUM I INTERFACE

by

CONSTANTINE ANTONOPOULOS

A thesis submitted in partial fulfillment of the
requirements for the degree of

MASTER OF SCIENCE


in

PHYSICS

Portland State University
1974

TO THE OFFICE OF GRADUATE STUDIES AND RESEARCH:

The members of the Committee approve the thesis of
Constantine Antonopoulos presented May 15, 1974.


Laird C. Brodie, Chairman


David W. McClure


Cecil E. Sanford


Jack Semura

APPROVED:


Makoto Takeo, Acting Head, Department of Physics


David T. Clark, Dean of Graduate Studies and Research

May 15, 1974

ACKNOWLEDGMENTS

I would like to express my gratitude to the following persons for their time and energies in order that this thesis might be a success.

To Mr. Sanford and Dr. Dash for their assistance with the evaporations. To Dr. Semura and John Opsal for their advice on the theoretical aspects of the work. And to Mr. Jack Janacek and the shop personnel for the construction of the holders.

In particular I would like to thank Dr. L. C. Brodie, for his invaluable help and guidance, without which, this thesis would have been impossible.

TABLE OF CONTENTS

PAGE

ACKNOWLEDGMENTS.....	iii
LIST OF TABLES.....	iv
LIST OF FIGURES.....	v
CHAPTER	
I INTRODUCTION.....	1
II EQUIPMENT.....	11
III THE SAMPLES.....	18
IV EXPERIMENTAL PROCEDURE.....	32
V RESULTS AND DUSCUSSION.....	38
VI CONCLUSIONS AND RECOMMENDATIONS.....	55
LIST OF REFERENCES.....	58

LIST OF TABLES

TABLE	PAGE
I Potentiometric data of Allen-Bradley carbon resistors at room temperature....	39
II Potentiometric data of Allen-Bradley carbon resistors at liquid helium temperature.....	39
III Experimental values of I , ΔV , and ΔR , where $\Delta R = (1/8)(\Delta V/I)$	42
IV Data obtained from the pumping down procedure.....	43
V Values of ΔR and $-\Delta T$ for the construction of the calibration curve.....	44
VI The temperatures of the sample as they were obtained from the calibration curve and the corresponding currents.	46

LIST OF FIGURES

FIGURE	PAGE
1. Simplified circuit for measurements of the magnetoresistance of bismuth crystals.....	2
2. Magnetoresistance of bismuth as a function of current for bath temperatures greater than T_1	2
3. Magnetoresistance of bismuth as a function of current for bath temperatures less than T_1	2
4. Typical overshoot.....	4
5. The sharp break.....	6
6. Decreasing peak effect.....	7
7. λ -sequence.....	8
8. Experimental environment.....	12
9. Main circuit logic.....	13
10. Switch box circuit diagram.....	14
11. Pulser circuit diagram.....	15
12. Temperature profile in the sample for different thicknesses.....	20
13. Typical carbon sample.....	21
14. Resistance of Allen-Bradley carbon resistors at low temperatures.....	22
15. Flattened Allen-Bradley carbon resistor	24
16. Model of carbon sample support.....	24
17. A carbon film sample with one scratch..	26
18. A carbon film sample representing the shape of the scratch.....	26
19. A diagram of the sample's holder.....	31

FIGURE	PAGE
20. Representation of amplifier balance.....	33
21. Representation of crystal balance.....	34
22. Typical scope traces of the output of amplifier #4, for currents less than 95mA.....	40
23. Scope trace of the output of amplifier #4 for currents greater than 95mA...	41
24. The calibration curve.....	45
25. Density of liquid helium as a function of the distance r from an immersed surface.....	52
26. Diagram for a possible explanation of the overshoot.....	52

INTRODUCTION

The subject to be discussed in this thesis is an experimental problem in heat transfer across a carbon-liquid helium I interface. The interest in this particular problem arose from experimental work first presented by Luce (1) concerning a similar heat transfer problem from a heated bismuth surface immersed in liquid helium. This study produced some interesting results which it was hoped could be duplicated with carbon. The choice of carbon as an alternative material was based on reasons which will be discussed later. Before beginning a detailed discussion of the problem a history of its development and the results which were obtained using bismuth single crystals will first be presented.

Several years ago, an experimental study of galvanomagnetic properties of pure bismuth at low temperatures was in progress. A partial requirement in the experiment was the measurement of the magnetoresistance and the Hall coefficient of bismuth. The bismuth crystal was part of a series circuit (Fig. 1) fed by a set of batteries. The crystal itself was in a dewar which contained liquid helium and placed between the poles of a magnet in such a way that the magnetic field was perpendicular to the flat surface of the crystal.

The measurements were taken when a DC current was flowing through the circuit. It was expected that both

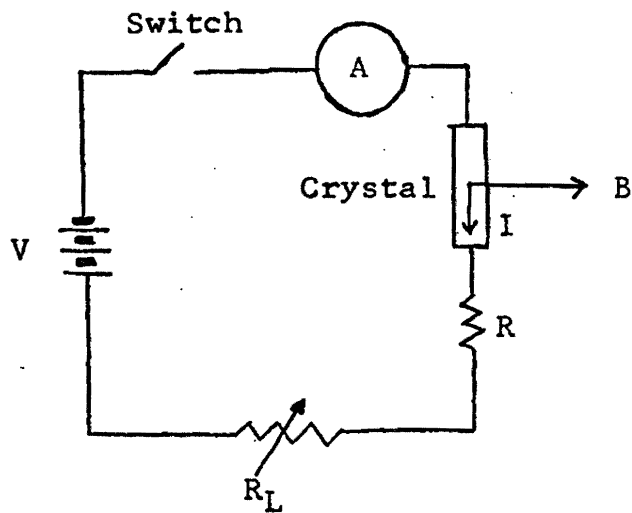


Fig. 1. Simplified circuit for measurements of the magnetoresistance of bismuth crystals.

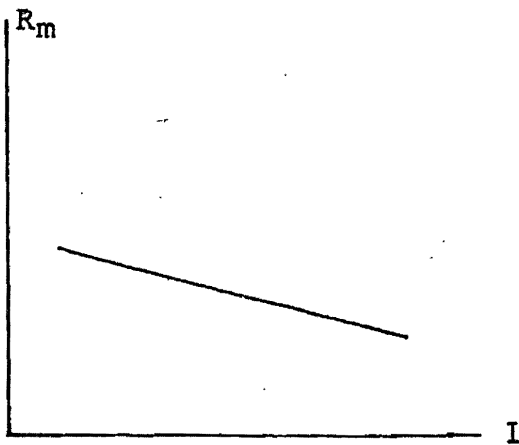


Fig. 2. Magnetoresistance of bismuth as a function of current for bath temperatures greater than T_λ .

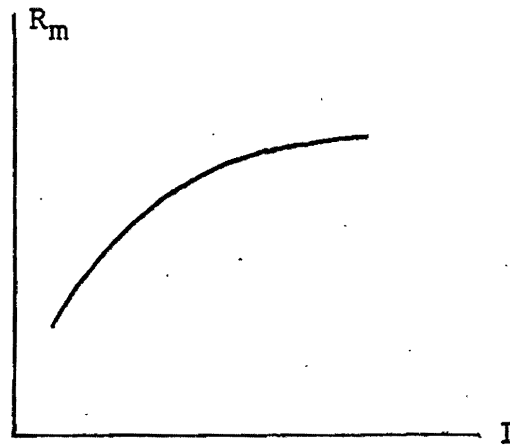


Fig. 3. Magnetoresistance of bismuth as a function of current for bath temperatures less than T_λ .

magneto-resistance and Hall coefficient would not be current depended. However the results of the experiment showed the opposite to be true. A plot of experimental data is represented in Fig. 2, and in Fig. 3.

In Fig. 2 the temperature of the helium bath was greater than T_{λ} (temperature corresponding to the λ -point of helium) while in Fig. 3 the bath temperature was less than T_{λ} . Since the magneto-resistance is a monotonically decreasing function of temperature the above results gave rise to confusion because according to Fig. 2 the crystal was being heated while according to Fig. 3 the crystal was cooling, as the current through the crystal was increasing.

It was thought at this time that this strange behavior of the bismuth crystal was due to the combination of some sort of thermal effect plus an intrinsic solid state non-ohmic effect. If this were the case then it should be possible to separate the thermal effect from the intrinsic non-ohmic effect by using a current pulse instead of DC current. This reasoning was based on the expectation that the thermal effects should build up more slowly than the electric effects. Therefore, it was thought that if one were to observe the time development of the pulse across the crystal, the influence of the thermal and electric effects on the shape of the pulse would be seen to take place at different times.

A current pulse was then passed through the crystal in an effort to separate the thermal effect. At the same

time the difference ΔT of the surface temperature of the crystal, minus the bath temperature was recorded as a function of time. ΔT was expected to increase monotonically up to a steady state value, but contrary to expectations ΔT was seen to "overshoot" before it reached the steady state value (Fig. 4).

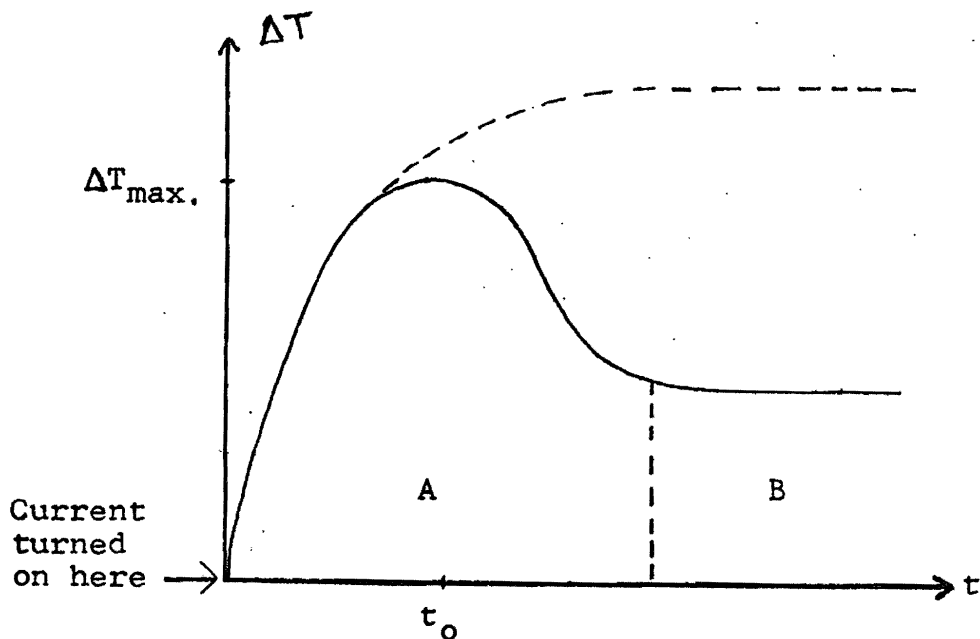


Fig. 4. Typical overshoot

In Fig. 4 it is seen that initially ΔT increases to a certain value ΔT_{\max} , corresponding to an elapsed time t_0 , after which it drops down, reaching a steady state value lower than expected.

The accidental discovery of the behavior of ΔT , transferred the research interest to the study of this "overshoot".

Before continuing, it was necessary to be certain that

the "overshoot" was not a result of the equipment. The electronics were examined exhaustively and found not to be the cause of the overshoot. A systematic study of the behavior of ΔT began.

The experimental set up was essentially the same as for the DC measurements except that provision was made for observing voltages immediately after the current was turned on. A standard resistor R_s was in series with the bismuth crystal and a current pulse was passed through the system. The difference ΔV , between the voltage V_R across two longitudinal leads on the bismuth crystal, and the voltage V_s across the standard resistor was displayed on the screen of a storage oscilloscope. A typical trace on the scope's screen is represented by Fig. 4.*

The regions A and B in Fig. 4 represent the transient and the steady states respectively. The typical time required for ΔT to reach steady state is up to 100 or 150 msec while the typical time in which ΔT reaches maximum is up to 50 or 60 msec. As it turns out the above numbers depend on the power which passes through the system.

As the applied power was increased the scope trace for ΔT changed from the initial smooth curves to a sharp break when a critical power input of approximately 30 mwatts/cm² was applied. Moreover the peak of the curve was trans-

* As will be explained later the behavior of ΔT is substantially the same as the behavior of ΔV seen on the scope, so that the trace in Fig. 4 can serve as an illustration of either ΔV or ΔT .

lated to the left (earlier time) as the power was increased. It should be emphasized however that the value of ΔT when the sharp break occurred was constant for all power inputs above the threshold of 30 mwatts/cm². (Fig. 5).

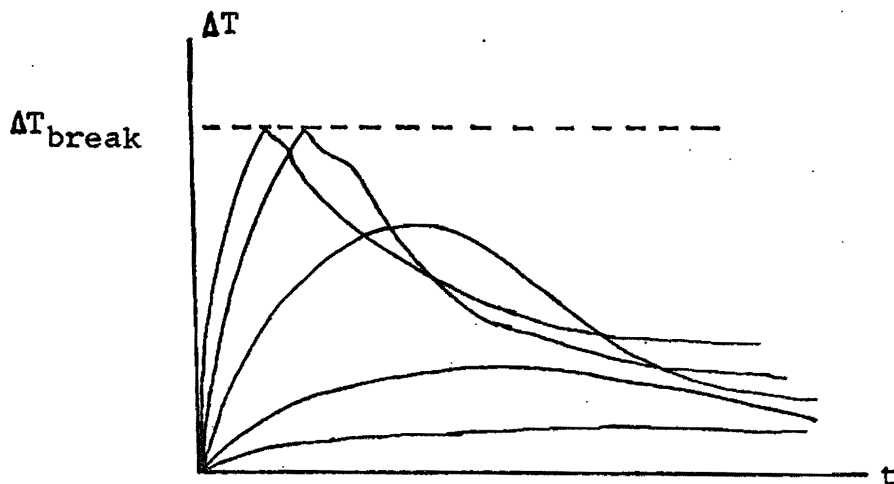


Fig. 5. The sharp break.

At the sharp break, ΔT was approximately equal to .3K and it occurred after an elapsed time less than 20 msec. In addition two more observed effects should be mentioned. The first is the so called "decreasing peak effect". If the ΔT 's corresponding to two or more successive pulses are observed after a long absence of power, the largest overshoot always corresponds to the first pulse. This effect is shown schematically in Fig. 6.

The second effect was tentively named " λ -sequence effect". This effect consists of the following: if the pressure of the helium vapor in the dewar is decreased, by pumping down on the system the temperature of the helium

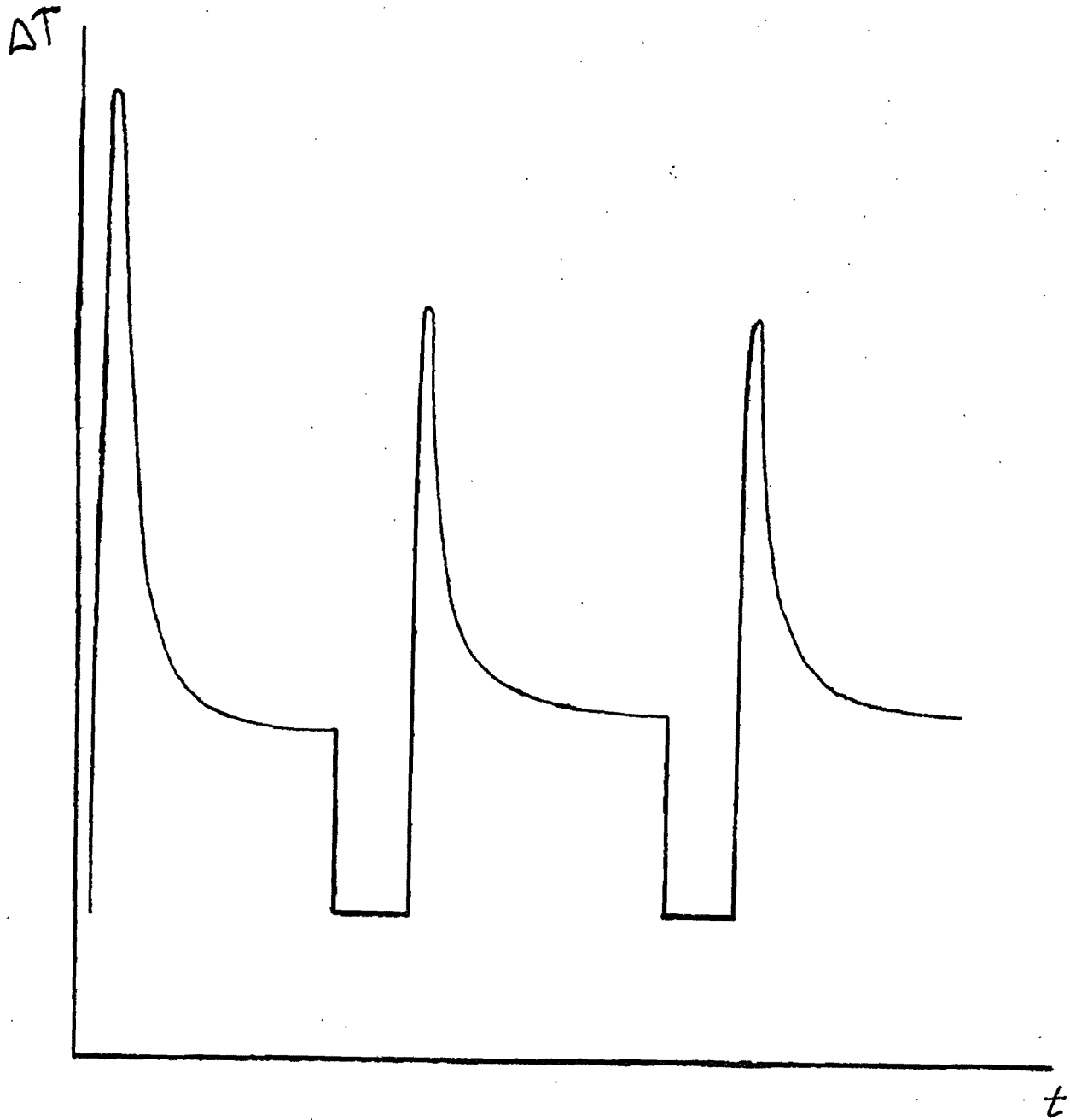


Fig. 6. Decreasing peak effect.

bath decreases, and as the helium passes through the λ -point the scope picture undergoes a sequence of successive changes. When the temperature falls below the λ -point, no heating of the crystal can be observed. (Fig. 7).

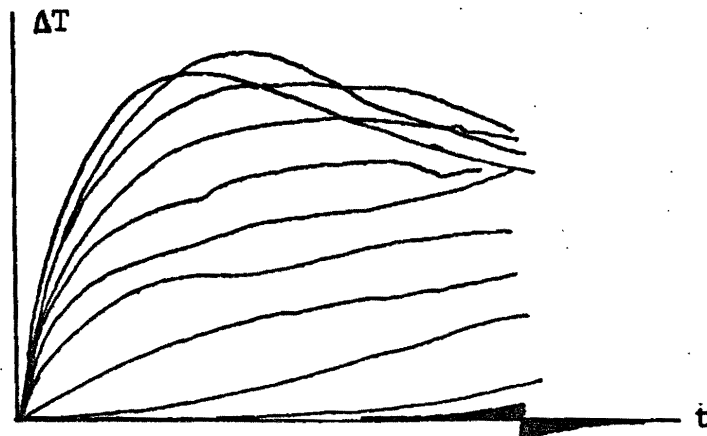


Fig. 7. λ -sequence

Summary of experimental results with bismuth:

1. ΔT overshoots before it reaches a steady state value
2. Sharp break of ΔT for power inputs more than 30 mwatts/cm².
3. Decreasing peak effect.
4. λ -sequence effect.

For an understanding of the experimental results it was necessary to invent a cooling mechanism able to extract sufficient amounts of heat from the surface of the crystal. The obvious cooling mechanisms of conduction and natural convection did not seem to be sufficient to account for the observed overshoot.

Smith and Giventer (2) have reported a similar temp-

erature overshoot on an analogous heat transfer problem from an electrically heated platinum wire immersed in liquid nitrogen. They suggested that the overshoot might be caused by the delayed onset of nucleate boiling, according to which bubbling takes place from distinct points or nuclei on the heated surface. The surface of the solid on microscopic scale is covered by all sorts of pits and cavities in which helium vapor is trapped. In such a case there exists in each cavity a vapor-liquid interface. Since the helium bath is at its boiling point as the crystal is heated a microscopic layer of liquid right next to the heated surface becomes superheated. Therefore evaporation of the liquid occurs across the vapor-liquid interface. This causes a vapor bubble to grow and finally depart from each active cavity. The procedure is then repeated with a certain frequency. Each bubble carries a certain amount of heat (the heat of vaporization) so that the overall effect is the extraction of a considerable amount of heat from the heated surface. For more details about nucleate boiling and boiling heat transfer correlations refer to (3, 4, 5).

In terms of nucleate boiling the overshoot can be explained qualitatively. In the beginning of the heating process when the nuclei have not yet become active, the main cooling mechanism is conduction and natural convection. The temperature difference ΔT rises rapidly toward the peak. With increasing surface temperature the nuclei become active and nucleate boiling begins. Due to this

onset of boiling the sample cools, and ΔT falls back to a steady state value below that which would have occurred without boiling.

The understanding of the sharp break effect is very poor. It might be that at high power inputs many nuclei become active simultaneously, but this is questionable. The decreasing peak effect is probably related to a hysteresis effect first reported by Reeber (6). It is connected with the fact that some nuclei remain active after the power is turned off so there is no delay time for these nuclei to start bubbling when the power is turned on again.

Finally, as far as the λ -sequence effect is concerned, below 2.18 K the liquid helium is in phase II. Due to its superfluid properties, liquid helium II is able to rapidly extract heat from the surface of the crystal and therefore the temperature of the crystal cannot be raised above the bath temperature.

The results presented above and the ideas associated with them appeared to be satisfactory. However it was suggested that possibly the results were due to the magnetic field. It was argued that what was being observed was a result of some sort of electromagnetic effect rather than the mechanism presented above. Therefore, it was necessary to show that the overshoot and associated effects could be observed in the absence of a magnetic field and the present work was undertaken with this objective in mind.

EQUIPMENT

Dewars and vacuum system

The temperature environment is provided by a double dewar (Fig. 8). The internal diameters of the outer and inner dewars are approximately 10 cm. and 5 cm. respectively. The liquid helium is contained in the inner dewar which is surrounded by the liquid nitrogen contained in the outer dewar.

A large capacity Kinney pump is connected to the inner dewar to lower the vapor pressure and hence the temperature of the helium bath.

Finally there are two pairs of parallel manometers to provide a convenient temperature measurement. For high pressure measurements a mercury filled tube was used with a vacuum on one side of approximately 50 microns. At lower temperatures an oil filled manometer could be connected in parallel with the mercury manometer. It was found that the oil height was 13.68 times the mercury height (see Fig. 8).

Electrical circuitry

The main electrical circuit is simple at least in principle (Fig. 9, Fig. 10). The power for the circuit was always supplied by the same set of batteries, but the current could be channeled through a pulser (Fig. 11) instead of directly to the crystal, so that it could be

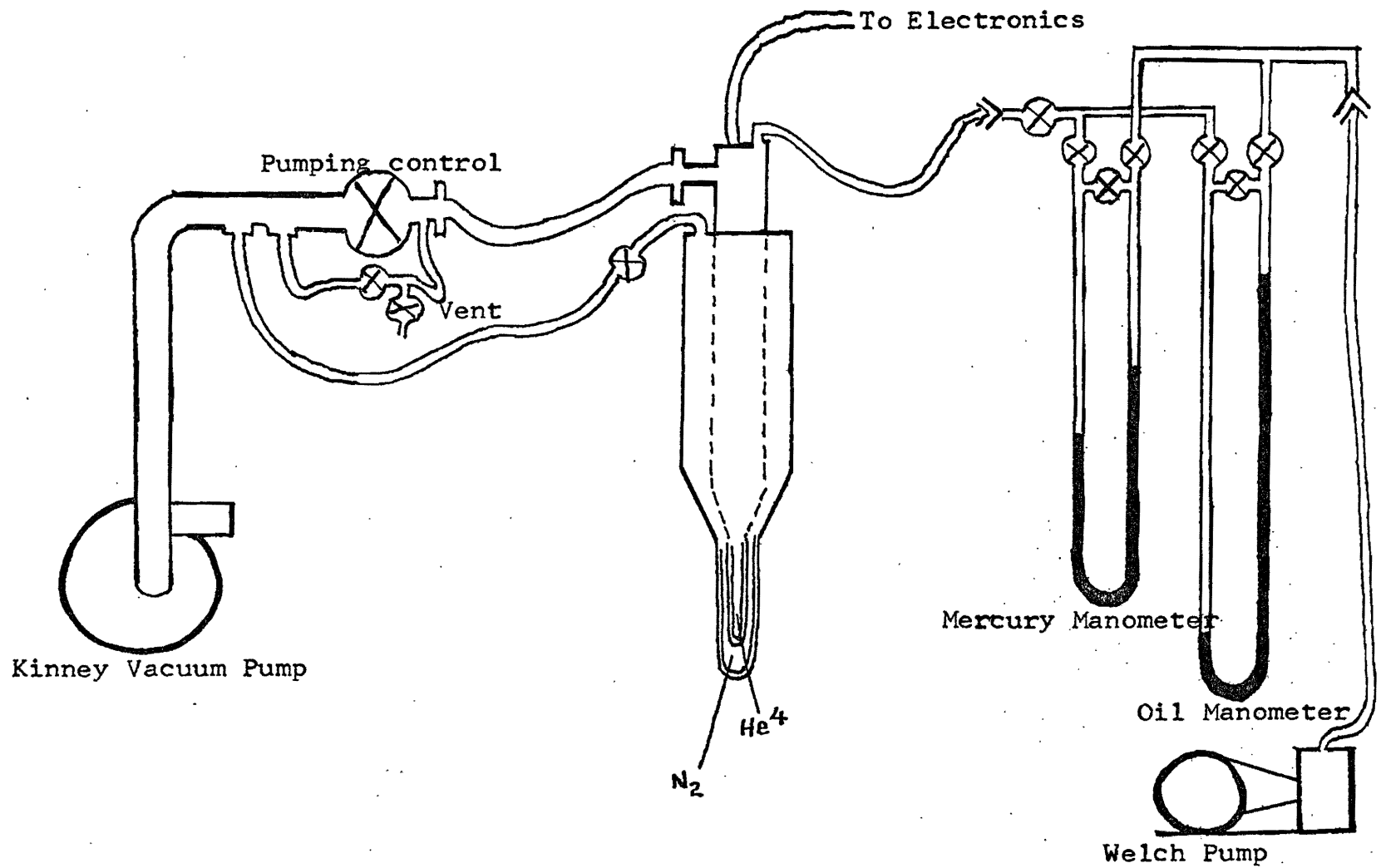


Fig. 8. Experimental Environment.

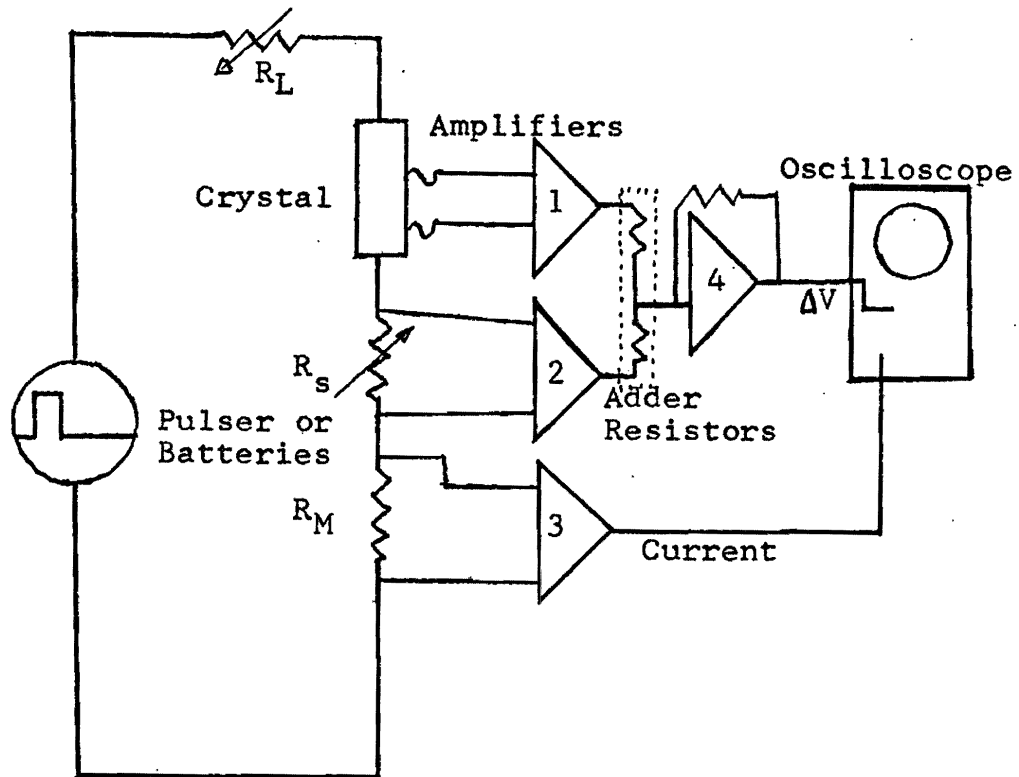
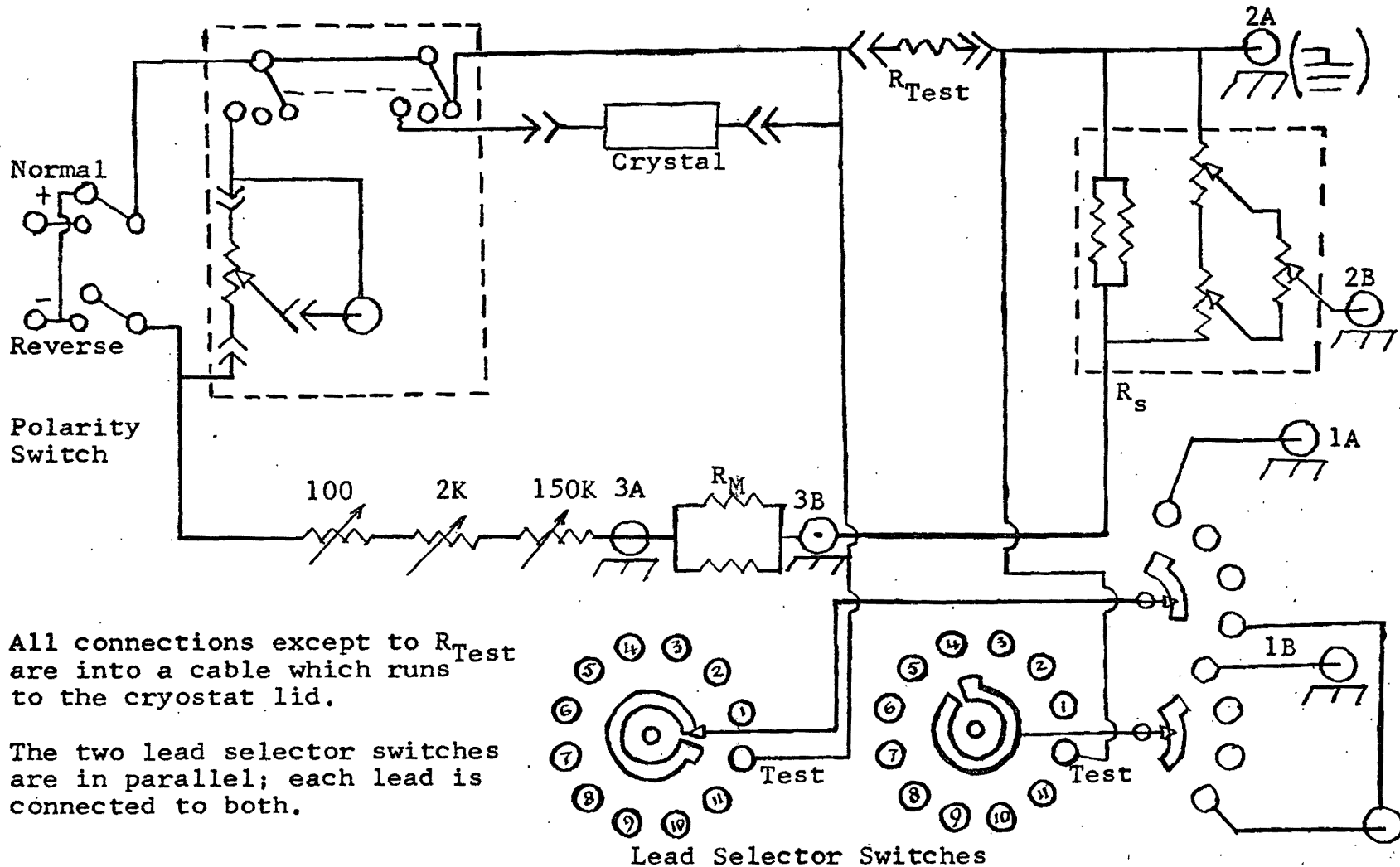


Fig. 9. Main circuit logic.



All connections except to R_{Test} are into a cable which runs to the cryostat lid.

The two lead selector switches are in parallel; each lead is connected to both.

Fig. 10. Switch box circuit diagram.

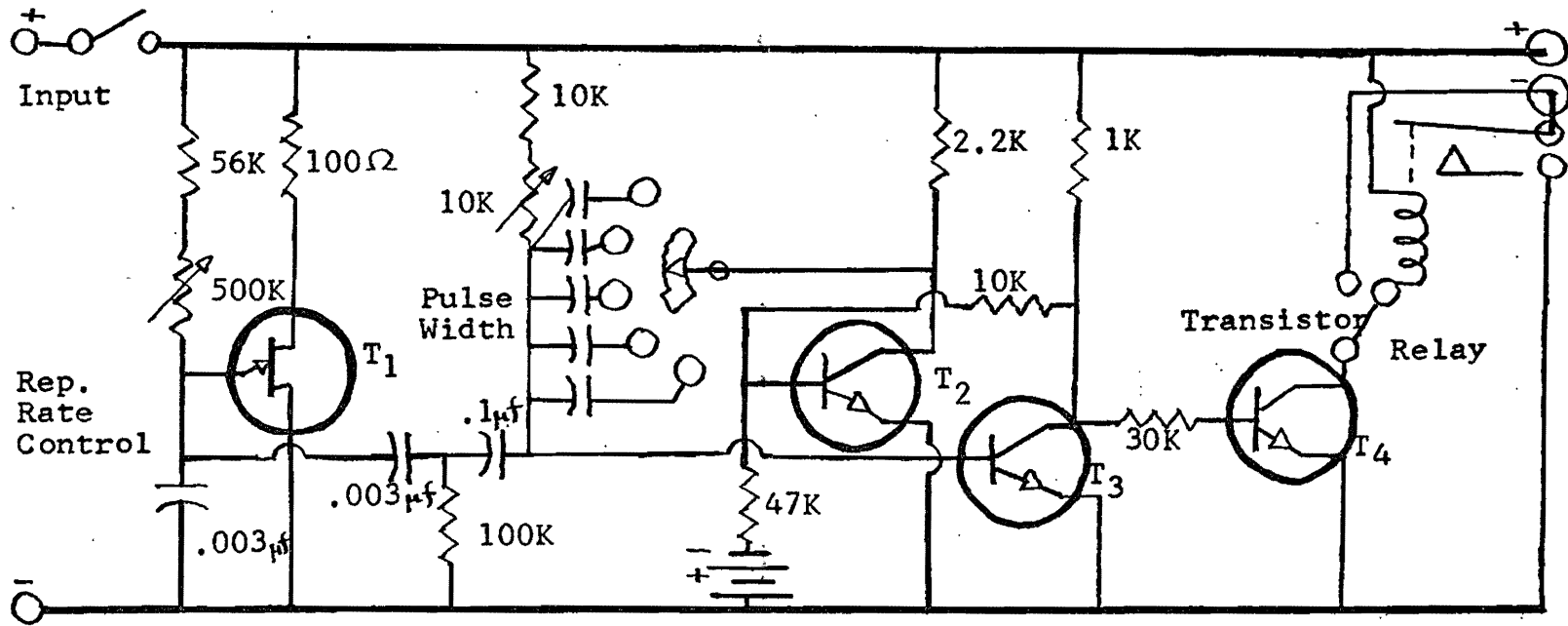


Fig. 11. Pulser circuit diagram.

switched on automatically as well as manually.

The current in the circuit is limited by the large variable resistor R_L and flows through a precision resistor R_M . The voltage from R_M is fed to the input of amplifier #3, a Burr Brown instrumentation amplifier model 3061, which is calibrated to give an output of 1/20th of a volt for each mA of current. In this way we were able to measure the current flowing in the circuit.

R_s is a source of voltage which follows Ohm's law and which can be compared to the voltage from the crystal. The latter is done by subtracting the linear voltage from R_s from the crystal voltage and after appropriate amplification displaying the difference on an oscilloscope with respect to time.

It is important to make certain that effects in the standard resistor R_s do not mask or change the apparent behavior of the sample. Therefore a metal film resistor, of low inductance and temperature coefficient of 25 parts per million per degree Celsius was adopted. In parallel with this a voltage divider was used to enable the operator to balance the crystal voltage exactly at a certain crystal temperature (crystal balance procedure). Since a fine control was needed the primary voltage divider was constructed of a pair of gauged ten-turn potentiometers, and a third ten-turn potentiometer was connected across their center taps.

The output from R_s is presented to the input of a

Burr Brown instrumentation amplifier model 3061 (amplifier #2 in Fig. 9, Fig. 10) which is calibrated to a gain of 2. The voltage from the crystal leads under examination is sent to the input of a third Burr Brown 3061 amplifier (amplifier #1 in Fig. 9, Fig. 10) the gain of which was adjusted at the time of the reading to match precisely that of amplifier #2. The outputs of these amplifiers are subtracted and the resultant voltage is sent to the inverting input of the final amplifier (amplifier #4 in Fig. 9, Fig. 10) which is a Burr Brown model 3009 amplifier, calibrated to a gain of 4. The 3061 amplifiers are differential types, with input impedances of approximately 50 megohms and exceptional stability, while the 3009 is a somewhat less sophisticated operational amplifier with an input impedance of about 50 kilohms.

The scope was a Tectronix storage oscilloscope model 564B. A 2B67 plug in time base was used and it was triggered by the current pulse from amplifier #3. The voltage axis was supplied by a type 3A3 plug in unit which is an accurately calibrated dual trace set of differential amplifiers.

Finally a Leeds and Northrup K-3 potentiometer was used to measure accurately the resistances of the used samples.

THE SAMPLES

Since the problem of the construction of the samples is of fundamental importance, it was decided to treat it separately.

The first problem was to find a material with which to replace bismuth. This material had to satisfy the following conditions:

- 1) The material's electrical resistance should be sensitive to temperature changes so it could be used as its own thermometer
- 2) The material should be such that the temperature distribution throughout the sample is fairly uniform. Under this condition it should be possible to satisfactorily approximate the surface temperature to the temperature of the bulk of the sample.

There were three alternative material sources; metals, semi-metals, and semiconductors.

The electrical resistance as well as the magnetoresistance of metals turns out to be too small both at room and liquid helium temperatures. In addition the resistance of metals at liquid helium temperatures is in the region of the residual resistance which is independent of temperature. For these reasons metals were eliminated without any further consideration.

The situation appears different in the case of semi-metals. The electrical resistance of semi-metals is still very small, but their magnetoresistance is larger and strongly temperature dependent, decreasing monotonically with temperature. Therefore they could be used for the temper-

ature measurement. Since bismuth itself is a semi-metal, our next best choice should be another semi-metal like antimony or arsenic. Nevertheless the most serious objection to using a semi-metal was the need of a magnetic field. It was necessary to avoid any possible effect of the magnetic field and consequently this category of materials was also eliminated.

Semiconductors were therefore left as the last source of materials to choose from.

In using a semiconductor there is no need of a magnetic field, since their zero field electrical resistance is large and temperature dependent at liquid helium temperatures. Moreover it was known that semiconductors were used successfully in low temperature thermometry so condition 1) stated earlier is satisfied.

The only disadvantage in using semiconductors seemed to be their poor thermal conductivity. The consequence of this would be that condition 2) could not be satisfied completely. Nevertheless this difficulty could be overcome by decreasing the sample's thickness (Fig. 12). Fig. 12 is representative of the temperature distribution throughout the sample. It is seen that a thin enough sample constructed from semiconducting material would serve the purpose.

From all possible materials belonging in this category carbon was chosen for the following additional reasons:

- 1) Carbon is easy to handle.

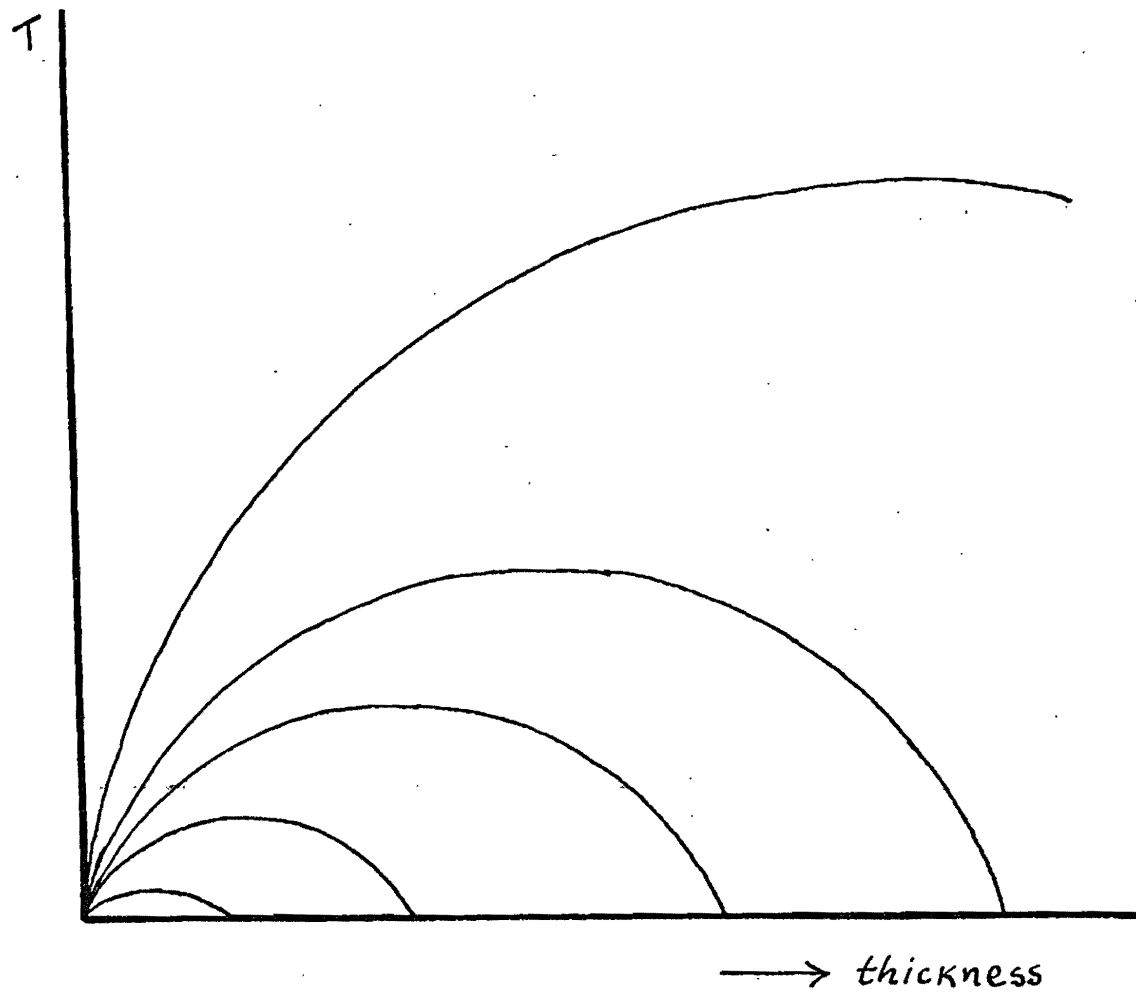


Fig. 12. Temperature profile in the sample for different thicknesses. Decreasing the thickness the temperature distribution becomes more uniform. The surface temperature has been chosen as zero.

- 2) One carbon film had already been tried.
- 3) The interactions between carbon and liquid helium are well known and this helps the quantitative theoretical analysis of the problem.

Handling carbon

The next step was to construct rectangular carbon samples several centimeters long, about one half centimeter wide and about one millimeter thick (Fig. 13).

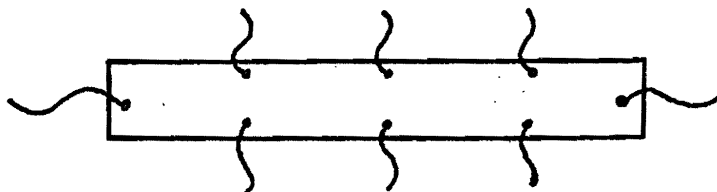


Fig. 13. Typical carbon sample.

Many different kinds of carbon were tried. Pieces were flattened down and given the proper shape with sand paper or other means. After the samples were cleaned, current and potential leads were attached by soldering thin copper wires. In some cases it was necessary to drill small holes in the specimens with an airbrasive unit in order to provide secure mechanical support for the lead wires.

The kinds of carbon originally used did not behave as sensitive enough thermometers. This became evident after the potentiometric measurements of the electrical resistance of the different samples at room and liquid

helium temperatures. They could hardly be considered as thermometers at all since their resistance while in the cryogenic liquid was changed by only a few percent with respect to their room temperature resistance. This behavior was unexpected and it was concluded that either not all carbons are good thermometers, or that the measurements did not only represent the electrical resistance of the carbon sample but in addition the contact resistance. Referring to the literature on the subject it was found (7,8) that Allen-Bradley carbon radio resistors were used as thermometers at low temperatures, particularly below 20 K, with good results. The figure below shows the temperature dependence of the electrical resistance of some Allen-Bradley resistors. (Fig. 14)

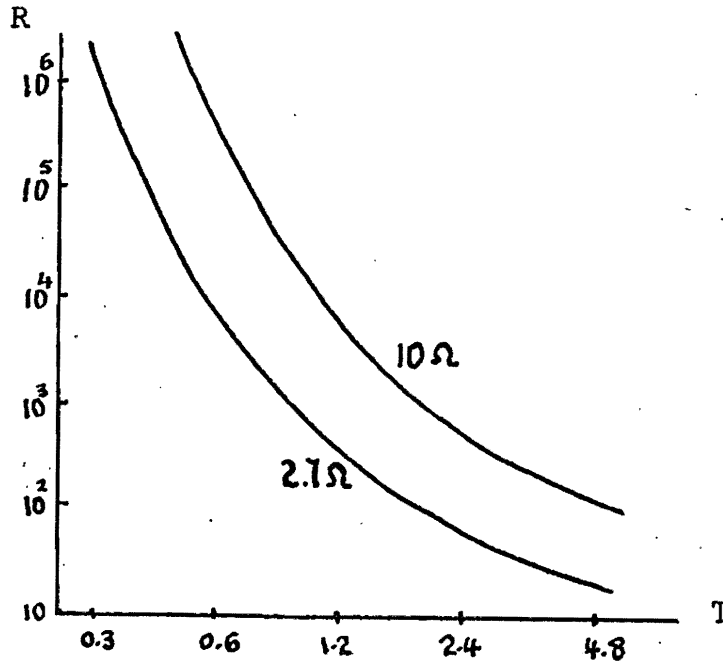


Fig. 14. Resistance of Allen-Bradley carbon resistors at low temperatures.

According to Fig.14, a 2.7Ω room temperature Allen-Bradley carbon resistor has about 30Ω resistance at 4.2 K. This is exactly what was needed since the equipment being used was designed to measure bismuth samples which were about 30Ω in liquid helium.

Several Allen-Bradley carbon resistors were flattened down carefully and were given a rectangular shape with dimensions in the range of a couple centimeters long, about .4 cm wide and roughly 1 mm thick. These carbon resistors already had two current leads attached so it was only a matter of attaching potential leads. One thin copper wire was soldered on each current lead. (Fig.15)

In doing so any additional contact resistance was avoided since the attachment was metal to metal. Minimal contact resistance still existed due to the fact that the manufacturer had attached leads to the carbon. The samples were then supported on a specially designed holder to prevent their motion and possible damage. (Fig.16)

Again potentiometric measurements of the electrical resistance at room and liquid helium temperatures showed that even these samples were still not very good thermometers. For example, a 9.7Ω (as it was measured at room temperature) Allen-Bradley carbon resistor was measured to have only 30Ω resistance at liquid helium temperature while according to Fig.14 a 10Ω room temperature Allen-Bradley resistor is expected to become over 100Ω in liquid helium.

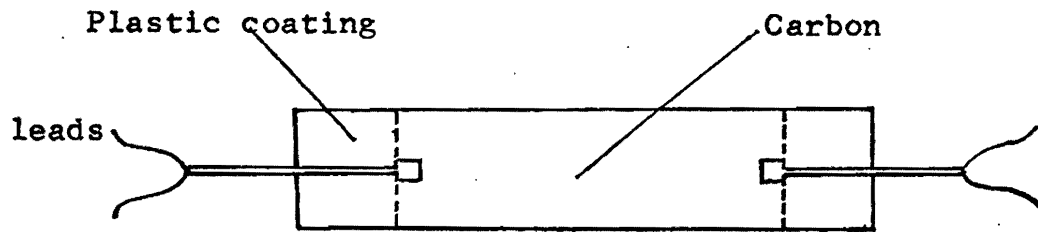


Fig. 15. Flattened Allen-Bradley carbon resistor.

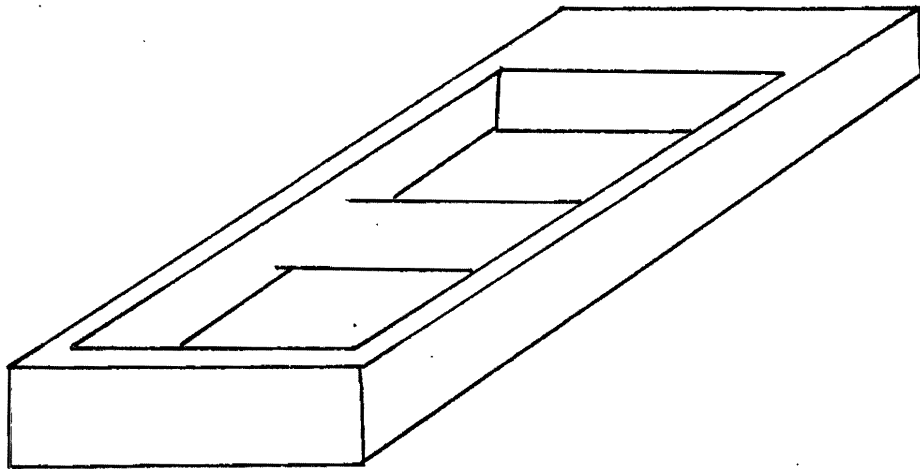


Fig. 16. Model of carbon sample support.

This contradiction led to the conclusion that the material from which the tested Allen-Bradley resistors were constructed differed from the carbon used in the 1950's, the date of the reference.

The resistance of the Allen-Bradley carbon resistor samples was about three times greater at 4.2 K than at room temperature.

Carbon films

Due to the fact that the Allen-Bradley carbon resistors were not very sensitive thermometers, together with the fact that their thickness could not be reduced indefinitely, a better carbon sample was looked for.

It was already known that an evaporated carbon film on a piece of mica or glass behaves as an excellent thermometer at low temperatures. However the resistance of such a carbon film was too high to be used as it was, and attempts were made to reduce its resistance.

Since $R \sim l/S$, where l is the length, and S the area of the cross section of the carbon film, its resistance could be reduced by changing its dimensions.

As far as the decrease of the length l of the carbon film is concerned the following was done. A silver film was first evaporated on a piece of glass, and using a needle a scratch was drawn, separating the silver film into two discontinuous parts. (Fig. 17). A carbon film was then evaporated on top of the silver, so that the glass was now

completely covered with first, a layer of silver, and second, a layer of carbon. The scratch however contained only a carbon layer. Leads were attached as shown in Fig. 17 so that the flow of current through the sample was as indicated by the arrows. The resistance of the sample would be practically the resistance of the carbon in the scratch only. Therefore if d is the length of the scratch along the direction of current flow the resistance was reduced by a factor d/l , with respect to the resistance of the sample in the case when it had been covered with carbon only (provided of course that the thickness t of the carbon film is the same). Still the resistance proved to be too high.

Attention was therefore turned towards the cross sectional area S . The cross sectional area equals: $S = a \cdot t$, where a is the width of the glass (and therefore of the carbon film) and t is the thickness of the carbon film. S can be increased by increasing a or t or both.

The width a could not be extended beyond a certain limit by increasing the width of the glass plate, since the sample soon became unusable, but the same result was achieved by changing the shape of the scratch. This time the scratch was not made straight, but rather as one continuous scratch moving back and forth across the sample many times, 100 times or more altogether (Fig. 18). This kind of scratch still divides the silver film into two discontin-

uous parts. Then a carbon film was again evaporated on top. Leads were attached at A and B, so that the direction of the current flow through the sample was as indicated by the arrows in Fig.18. The resistance of the sample was practically the resistance of the solid dark part of the figure where there is only carbon. If d is still the width of the scratch and a' is now its length the resistance is reduced further by a factor a/a' for the same carbon thickness. So altogether the resistance is reduced by a factor:

$$K = (ad)/(a'l)$$

Numerical values are given here for an estimation of K . If the dimensions of the glass are: $l = 4\text{cm}$, $a = 1.5\text{cm}$, and the dimensions of the scratch are: $d = 10^{-3}\text{cm}$, and assuming that the scratch is going back and forth n times, $2a$ cm distance each time, then a' is approximately equal to:

$$a' = a + 2na = (2n + 1)a$$

Therefore:

$$K = (d/l)(a/2n + 1)(1/a) = (d/l)(1/2n + 1)$$

For $n = 100$, $K = 10^{-6}$.

The resistance of a carbon film evaporated on a piece of mica had been measured to be of the order of $10^7\Omega$ at liquid helium temperatures, and the dimensions of the carbon film were about equal to the ones used in the above example. It should have been possible therefore to reduce the resistance of the carbon film to several ohms at liquid helium temperatures.

In practice trying to make a carbon film in the way described above turns out to be a difficult job, dictated by the limitations of the equipment.

A #1 (thickness) microscope cover glass about 4cm long and 1.5cm wide was used. The glass was cleaned first with soap and then it was rinsed with distilled water and alcohol so as to eliminate any grease on the glass. After this a thin silver film was evaporated on its surface. It was found that the best scratches resulted when the silver film was quite thin. The scratches were made on the silver film by moving a phonograph needle back and forth with the help of a milling machine. The width of the scratches was of the order of 10^{-3} cm. Finally on top was evaporated a carbon film, whose thickness was about 20 microns. The evaporation of carbon was performed under vacuum and a small cylindrical shaped rod of carbon was evaporated each time. Increasing the thickness of the carbon film was expected to further reduce the resistance. In practice though, the opposite effect was observed for most of the samples. The problem was that each time additional carbon was to be evaporated, a return to atmospheric conditions was necessary in order to replace the carbon rod in the evaporator. In this way probably the surface of the carbon film was oxidized by air. According to this explanation, a layer of oxide was created between each layer of carbon film, preventing direct contact between successive layers, adding extra contact resistance.

The possible oxidation process could be avoided by using an evaporator which would allow for several evaporations of carbon before a return to atmospheric conditions. Another explanation is that an oil film was deposited on the sample's surface preventing again direct contact between carbon layers.

Several samples were constructed and in some cases their resistance was reduced down to 4Ω at room temperature. Since the glass was very fragile, the samples were supported in a special holder (Fig.19) and two pressure contacts were made instead of attaching leads in any other way. Four leads were connected, two on each of the pressure contacts, resulting in a pair of current and a pair of potential leads.

The main disadvantage of these samples was their high resistance at liquid helium temperatures. A modification is necessary to reduce the value of their resistance while in helium by several orders of magnitude. A less serious disadvantage, is that the carbon film is exposed directly to the liquid only from one side. It has been reported (9) that in the case of glass substrates most of the heat is conducted directly into the helium bath, bypassing the substrate, but as far as boiling is concerned the effect of the substrate is to decrease the area of the sample available for nucleation.

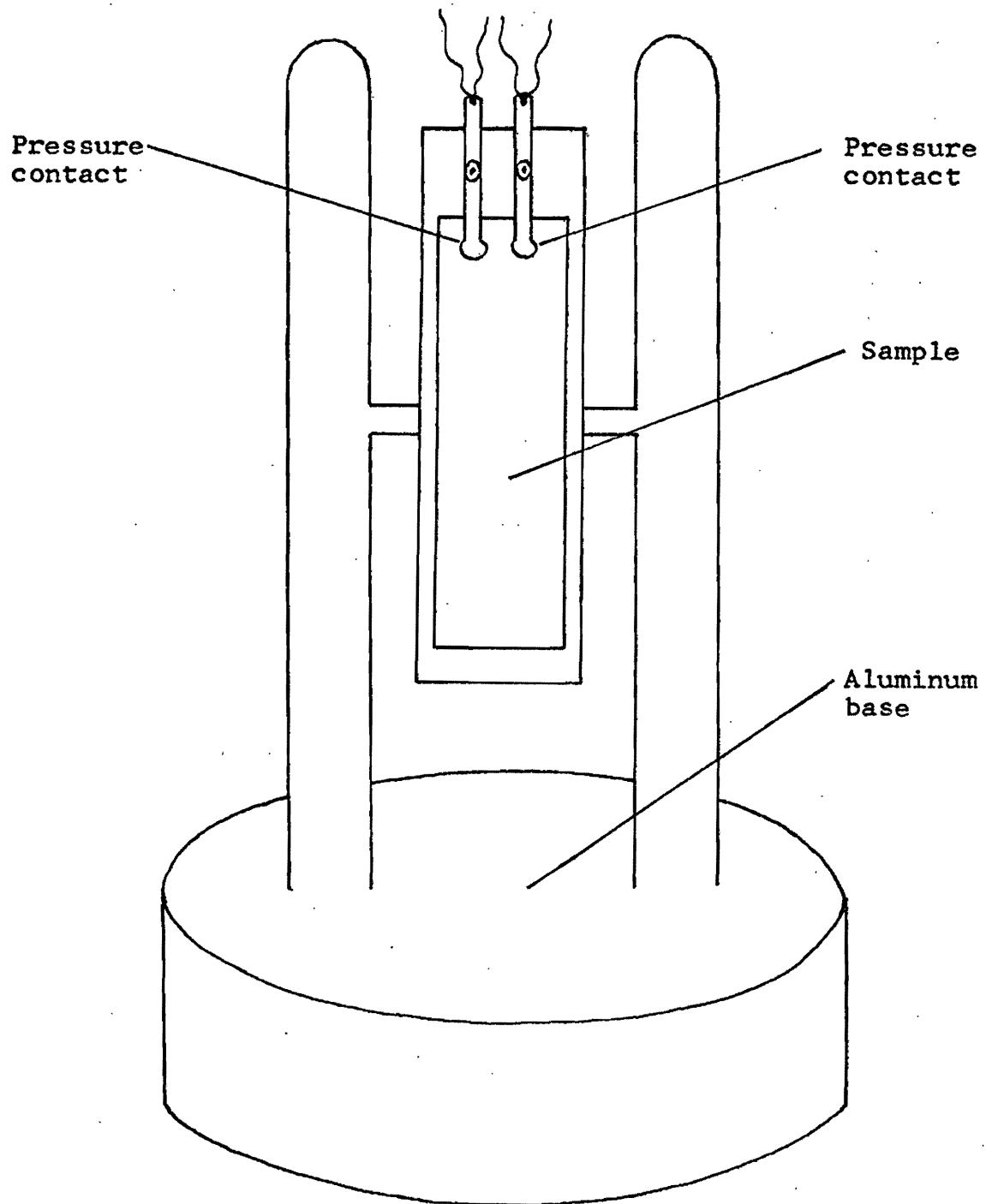


Fig. 19. A diagram of the sample's holder.

EXPERIMENTAL PROCEDURE

With the carbon samples placed in the inner dewar with their largest dimension vertical, the first step was to compare their room and liquid helium temperature resistances. The measurement of the sample's resistance was obtained with the use of a potentiometer which was standardized before every use. The current passing through the sample during this procedure was kept low enough to avoid any heating effects. The ratio of these two resistance values was then a measure of the ability of the sample to be used as its own thermometer.

The next and far more critical step was the temperature measurement of the sample under consideration. It should be noted again that when speaking about the sample's temperature, its surface temperature is what is really meant. This is a fundamental assumption and it is satisfied by good quality samples. With this in mind the temperature measurement or more precisely the difference ΔT between the sample's surface temperature and the temperature of the bath was the final result of the following set of operations.

1. Amplifier balance

The inputs of amplifiers #1 and #2 are connected together in reversed polarity and fed by the same pulse, coming not directly from the batteries but through the pulser. Since the gain of these amplifiers is the same, the signals in their outputs have the same magnitude but

they are reversed. The situation is represented schematically in Fig.20 below.

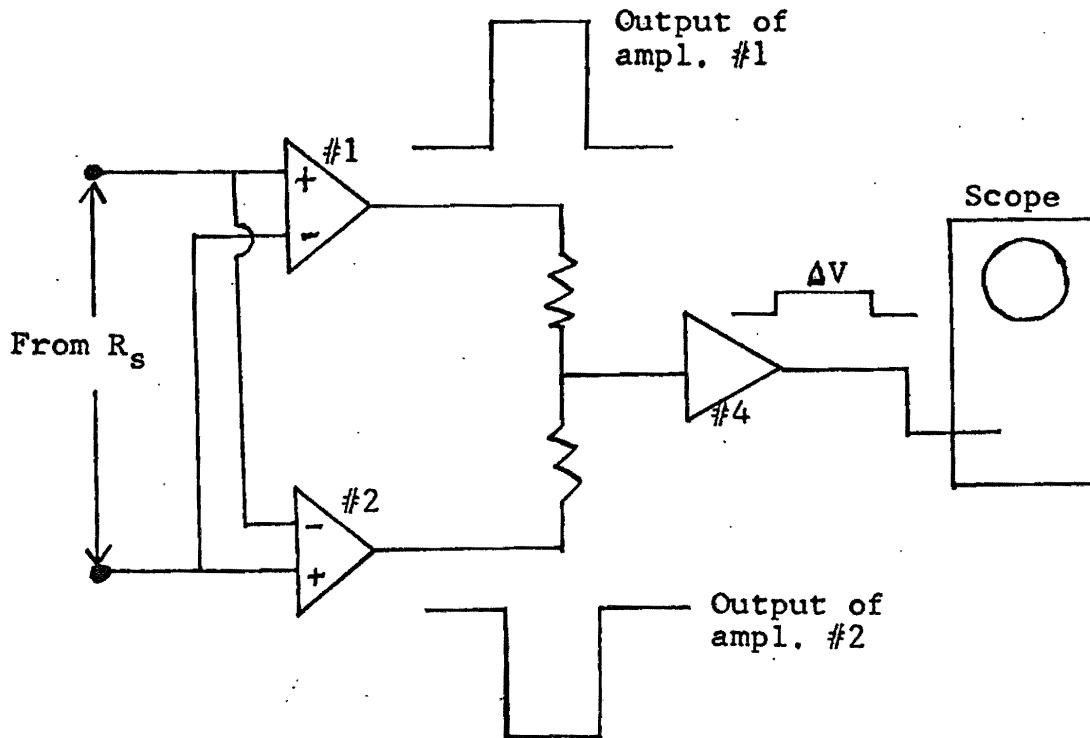


Fig. 20. Representation of amplifier balance.

Amplifier #4 then adds through the adder resistors, and simultaneously inverts and amplifies the sum of the two pulses. This sum can be displayed on the scope. The balance of amplifiers #1 and #2 consists in adjusting the gains of the amplifiers in such a way that the trace on the scope's screen becomes zero. This can be done to an accuracy of 0.1 mV. The amplifier balance is repeated at every run before the transfer of liquid helium into the dewar.

2. Crystal balance

This balancing procedure follows the previous one and takes place while the sample is in liquid helium. The use of the pulser is not necessary in this case. It is more convenient to simply hand-pulse the current through the system. Currents higher than 15 mA were used, so the warming of the sample could be readily seen.

The voltages across the carbon sample and the standard resistor R_s were fed into the inputs of amplifier #1 and #2 respectively, in reversed polarity. The shape of the pulses at the outputs of the amplifiers is represented in Fig. 21 below.

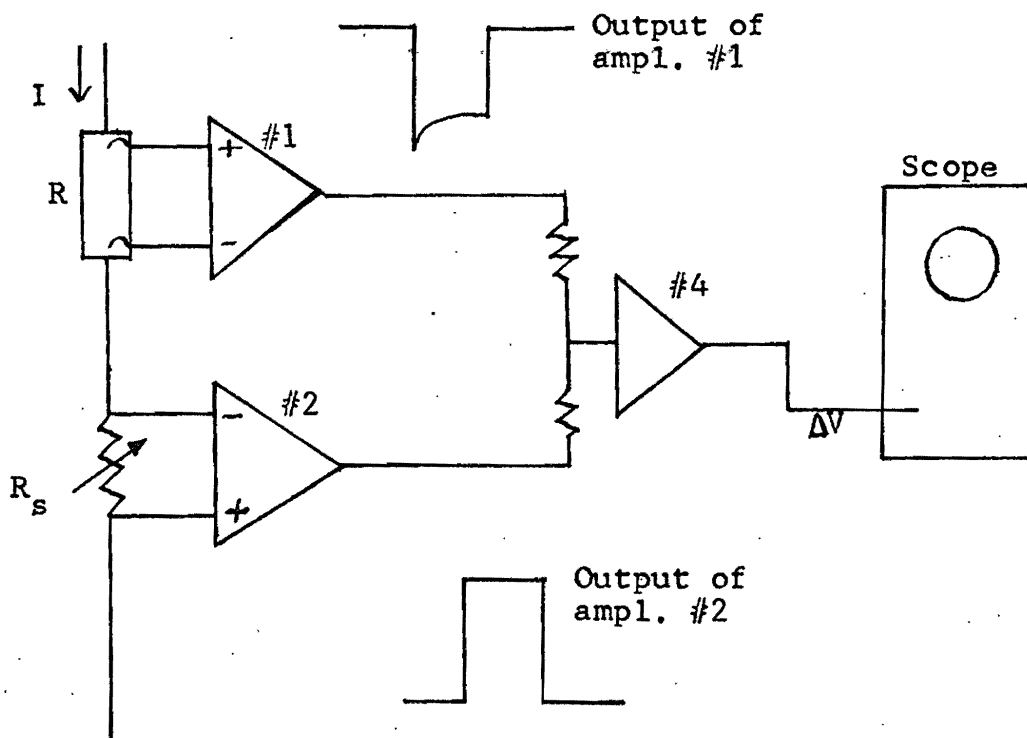


Fig. 21. Representation of crystal balance.

At the output of amplifier #2 the top of the pulse is flat because the voltage across R_s is constant, since R_s is a standard resistor and its resistance is temperature independent.

The situation is different at the output of amplifier #1. The current warms up the sample, and consequently its resistance decreases. As a result of this the voltage across the carbon sample decreases, at least at the beginning of the pulse. The crystal balance procedure consists in adjustment of the standard resistor R_s in such a way that the sum of the two pulses at the beginning is zero. Under this condition the trace of the output V_4 of amplifier #4 on the scope starts from zero.

Expressed quantitatively:

$$V_4 = V - V_s = IR - IR_s = 0, \quad \text{or;}$$

$$R = R_s \quad \text{at } t = 0.$$

From the above relation it is seen that in order to be able to crystal balance the magnitude of the standard resistor R_s must be at least equal to the resistance of the sample while in liquid helium.

As the time passes the resistance of the sample R , as well as the current I , flowing through the sample, change by amounts ΔR and ΔI respectively. Therefore for $t \neq 0$:

$$\begin{aligned} V_4 &= V - V_s = (I + \Delta I) \cdot (R + \Delta R) - (I + \Delta I)R_s = \\ &= I(R - R_s) + \Delta I(R - R_s) + I\Delta R + \Delta I\Delta R . \end{aligned}$$

The first two terms are zero due to crystal balance, while the fourth term is a correction which can be made as small as desired by increasing the battery voltage and the total resistance of the circuit. Neglecting this term:

$$V_4 = I \cdot \Delta R = \Delta V \quad (\tau \neq 0)$$

The voltage V_4 at the output of amplifier #4 represents the (amplified) change in the voltage of the sample at any time. From this dividing by the current value I , the change in the resistance of the sample during the entire pulse is obtained.

3. Temperature calibration

Upon completion of the preliminary steps the next is to calibrate the thermometer (the sample itself). The temperature calibration was done by measuring the voltage V_4 on the scope's screen as a function of the helium vapor pressure, as the system was slowly pumped down. The current was held constant during the entire procedure, and was kept small enough to avoid any heating of the sample. The temperature of the bath and of the carbon sample decreased as pumping down began, and as a consequence of this, the scope trace for V_4 appeared to be out of balance. The resistance change of the sample can be calculated from the formula: $\Delta R = \Delta V / I$, and the simultaneous helium vapor pressure can be calculated from the manometer readings. The temperature of the bath was obtained from the helium vapor pressure using the 1948 scale.

It was then possible to plot pairs of corresponding values ΔR , ΔT where ΔT is the difference of the actual bath temperature T , minus its original temperature T_b , at the normal boiling point ($T_b = 4.2$ K). Obviously ΔT is negative. Such a graph represents the temperature calibration curve in the region below the normal boiling point of helium and can be extended down to approximately 1.5 K.

In case the experiment is run with the helium bath at its normal boiling point, so that as the sample warms up its temperature exceeds 4.2 K, the calibration curve must be extrapolated into the positive ΔT plane. Since the temperature of the sample was not expected to increase very much, and the slope of the calibration curve turned out to be, generally speaking, fairly constant near zero, the calibration curve was extrapolated linearly in the direction of the straight line, which passes through zero and its slope equals the derivative of the curve calculated at zero. With the calibration curve the carbon sample becomes a thermometer.

RESULTS AND DISCUSSION

The carbon film samples were first checked in liquid helium but their resistance was found to be too high. Characteristically a carbon film with a resistance of 4Ω at room temperature possessed a resistance of approximately $6,000\Omega$ at liquid helium temperatures. These samples were very sensitive thermometers but with the available equipment it was impossible to run the experiment with them in helium since, due to their high resistance, they could not be heated.

The Allen-Bradley carbon resistors were then the only kind of samples left to try.

The resistance of the sample was the ratio of potentiometric values of the voltage across it to the current flowing through it. These values for a typical rectangular sample with dimensions, $1.14\text{cm} \times .36\text{cm} \times .1\text{cm}$, are tabulated in tables I and II for both room and liquid helium temperatures.

According to these tables the resistance of the carbon sample at helium temperatures increases by a factor 4.16 with respect to its room temperature resistance. For comparison it is stated at this point that in the case of bismuth and for a 15 KGauss magnetic field the ratio of the magnetoresistance values at helium and room temperatures respectively, is of the order of 10^4 . Clearly the carbon resistors are not as sensitive thermometers.

TABLE I

Potentiometric data of Allen-Bradley carbon resistors at room temperature.

$I \times 10^{-4}$ (A)	$V \times 10^{-3}$ (Volts)	R (Ω)
1.6785	1.3555	8.06
2.218	1.792	8.08
3.1365	2.5345	8.08
4.482	3.621	8.08

TABLE II

Potentiometric data of Allen-Bradley carbon resistors at liquid helium temperatures.

$I \times 10^{-5}$ (mA)	$V \times 10^{-3}$ (Volts)	R (Ω)
6.43	2.1635	33.65
13.254	4.4575	33.63
25.56	8.596	33.63
35.99	12.0006	33.62

Observation of the trace of ΔV and the possibility of seeing an overshoot was the main interest. The output of amplifier #4 was fed into the oscilloscope input and the sweep was triggered by the output of amplifier #3. The current could be increased up to approximately 95 mA. A 50Ω standard resistor was used for R_s . As the current was varied the resistance of the sample changed so that it appeared to be out of balance. Readjustment of R_s for crystal balance every time the current was changed was therefore necessary. Typical scope pictures of the output of amplifier #4 are represented in Fig. 22.

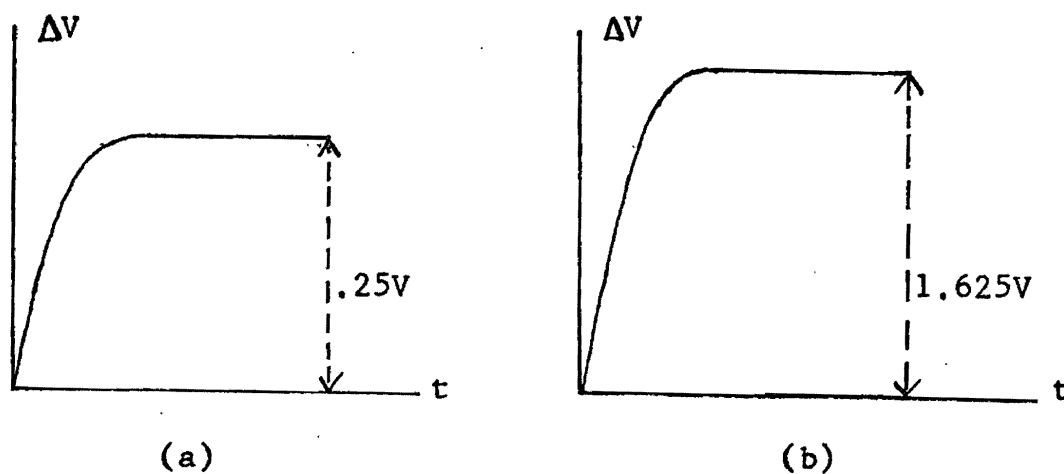


Fig. 22. Typical scope traces of the output of amplifier #4, for currents less than 95mA.

No overshoot was observed. ΔV rises monotonically up to a steady state value dependent on the applied power. In Fig. 22a and 22b, the values of the current were 25 mA and 90 mA respectively, while the corresponding steady state values for ΔV were .25 volts and 1.625 volts.

The time required for the steady state to be established was about 100 msecs and no appreciable change was observed with variation of the power.

Fig. 23 represents the trace ΔV of the scope for a current greater than 95 mA passing through the sample.

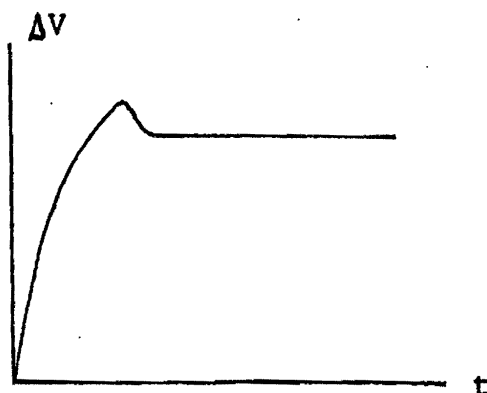


Fig. 23. Scope trace of the output of amplifier #4 for currents greater than 95mA.

Originally it was thought that the observed peak in Fig. 23 was the overshoot, but later it was found that the peak was a result of overdriving the amplifiers. This appeared to happen for currents greater than 95 mA.

The change, ΔR , of the resistance of the sample which is necessary for the determination of its temperature at steady state was found from the steady state values of ΔV and the corresponding current. Some of these values are tabulated in table III.

The pumping down procedure for the construction of the temperature calibration curve took place at the end of the experiment, when the liquid helium was just covering

TABLE III

Experimental values of I, ΔV and ΔR , where $\Delta R = (1/8)(\Delta V/I)$.

I (mA)	ΔV (Volts)	ΔR (Ω)
25	2.1	10.5
50	6.0	15.0
60	8.0	16.66
75	10.4	17.33
90	13.2	18.33
92.5	13.6	18.38

the sample. A small current ($I = .5$ mA) channeled through the pulser was flowing in the circuit. The values of the ΔV 's, the mercury manometer readings, and the bath temperatures obtained from the vapor pressure values using tables, are contained in table IV.

The values of the resistance change ΔR were calculated from the formula: $\Delta R = (1/8)(\Delta V/I)$, where ΔV are the values which appear in table IV, $I = .5$ mA, and the ratio $\Delta V/I$, is divided by the total amplifier gain of 8. The corresponding values of $(-\Delta T)$ were obtained by subtracting the actual bath temperature from the initial temperature 4.23 K. The values of ΔR and $(-\Delta T)$ appear in table V.

TABLE IV

Data obtained from the pumping down procedure.

ΔV (mV)	h_1 (cm)	h_2 (cm)	$h_2 - h_1$ (cm)	T °K
0	11.6	88.8	77.2	4.23
4	15.0	85.0	70.0	4.13
6	17.1	83.0	65.9	4.07
8	19.8	80.5	60.7	3.98
14	23.7	76.5	52.8	3.85
16	25.0	75.0	50.0	3.80
20	28.2	72.0	43.8	3.68
27	31.3	68.8	37.5	3.55
34	34.2	65.9	31.7	3.41
43	37.1	62.9	25.8	3.25
56	39.8	60.3	20.5	3.08
68	42.0	58.0	16.0	2.92
80	43.4	56.5	13.1	2.79
106	45.6	54.3	8.7	2.56
124	46.7	53.3	6.6	2.43
154	47.7	52.2	4.5	2.25
170	48.1	51.9	3.8	2.18
190	48.8	51.2	2.4	2.01
210	49.0	51.0	2.0	1.95
250	49.2	50.9	1.7	1.89

TABLE V

Values of ΔR and $-\Delta T$ for the construction of the calibration curve.

ΔR (Ω)	ΔT $^{\circ}K$	ΔR (Ω)	ΔT $^{\circ}K$
0	0	17.00	1.31
1.0	0.10	20.00	1.44
1.5	0.16	26.25	1.66
2.0	0.24	31.00	1.80
3.5	0.37	38.50	1.98
4.0	0.42	42.50	2.05
5.0	0.54	47.50	2.14
6.75	0.68	52.50	2.22
8.5	0.82	57.50	2.28
10.75	0.98	62.50	2.33
14.0	1.14		

From the values of ΔR and $(-\Delta T)$ the calibration curve was graphed. (Fig. 24).

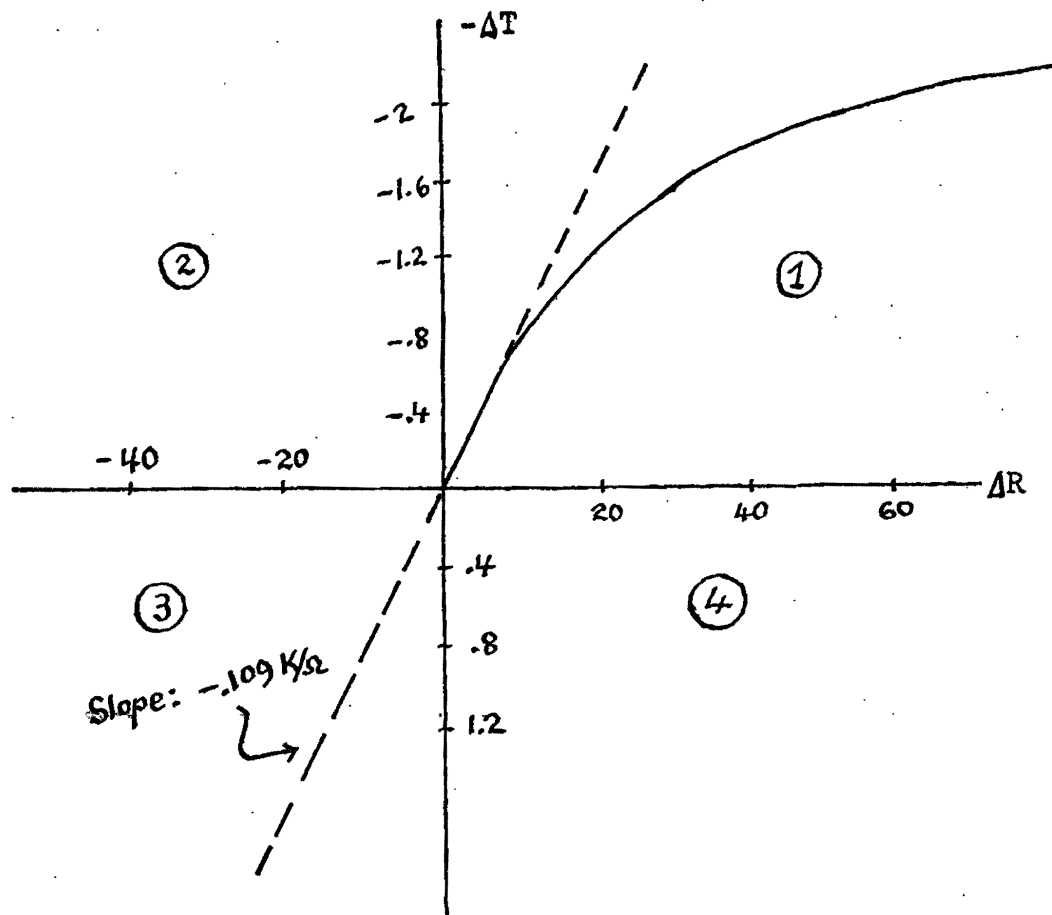


Fig. 24. The calibration curve.

The temperature of the carbon sample can be found by extrapolating the calibration curve into the third quadrant, and using the values ΔR , from table III. The slope of the calibration curve in the neighborhood of the origin is equal to:

$$(\Delta T/\Delta R)_0 = -.109 \text{ K}/\Omega .$$

Therefore the temperature of the sample can be calculated from the relation:

$$T = T - T_b = (\Delta T/\Delta R)_0 \cdot \Delta R, \quad \text{or}$$

$$T = T_b + (\Delta T/\Delta R)_0 \cdot \Delta R$$

where $T_b = 4.23$ K (normal boiling point of liquid helium) and ΔR are the values from table III.

The values obtained for the sample's temperature for the corresponding currents are given in table VI. Because of the linear extrapolation of the calibration curve to temperatures above 4.2 K, these values of T are only lower limits to the sample temperatures.

TABLE VI

The temperatures of the sample as they were obtained from the calibration curve and the corresponding currents.

I (mA)	T °K
25	5.37
50	5.86
60	6.04
75	6.12
90	6.23

The measured values for the sample's surface temperature exceed the critical temperature T_c , of helium ($T_c = 5.2$ K). Because of this unexpected result it was thought that the temperature being measured was not the actual surface temperature of the sample. The only conclusion which seemed reasonable was that the sample failed to satisfy the fundamental condition 2) as described in the section titled "The Samples". The 1mm thickness of the carbon sample appeared to be too great to allow the establishment of a uniform temperature distribution throughout.

In an attempt to verify this idea the output ΔV of amplifier #4 when the helium bath was above the λ -point was compared with the corresponding ΔV at bath temperatures below λ -point, under constant power input. Adjusting R_s so that the scope's trace for ΔV was readily visible at 4.2 K, pumping down began and continued to lower the bath temperature down to 1.9 K. No change was observed in the general shape of the heating curve, even when the λ -point was passed. It is known that upon reaching the λ -point, the liquid helium I undergoes the so called λ -transition and becomes superfluid helium II. As a result of this transition the properties of the liquid change dramatically. In particular its thermal conductivity increases by several orders of magnitude and consequently the liquid is able to extract heat more efficiently. Since it was supposed that the temperature measurements were representing the surface temperature of the sample, it was logical

to expect some change of the scope's trace as the bath temperature fell below λ -point. Contrary to expectations no appreciable change was observed, which again can be connected with lack of uniform temperature distribution in the sample due to low thermal conductivity of carbon.

If this idea is accepted then from the results of the experiments it cannot be concluded that the surface temperature does not overshoot before it reaches a steady state value. Since nothing is so special about bismuth as far as nucleate boiling is concerned, it was assumed that this basic cooling mechanism operates in the case of carbon samples too. Although it might be expected that bubbles could be observed to rise from the heated carbon surface, they were not visible, at least with the naked eye. They are probably too small or their life was too short to be seen (after all they were not visible in the case of bismuth either).

According to our understanding the existence of nucleate boiling causes the overshoot of the surface temperature which should be detectable with a favorable type of carbon sample. If this argument is essentially correct, then it is very possible that the overshoot really exists but it is hidden. It may be that the carbon samples employed were not sensitive enough to detect this change of the surface temperature. Therefore the inadequate quality of the carbon samples seems to be responsible for the negative results of the experiment up to this point.

When considered from a slightly different point of view, the reason that the carbon samples failed becomes clearer.

At very low temperatures the effect of the finite propagation speed of heat flowing through a material becomes more important. As a result of this, the function which describes the temperature distribution in the bulk of the material contains a time factor e^{-Dt} , where D is a characteristic of the material called thermal diffusivity. The inverse of D has dimensions of time and characterises the "relaxation time" of the system. The relaxation time τ , which is a measure of how fast a temperature change in some region of the material propagates through different regions in the material, can be expressed as:

$$\tau \sim D^{-1} = c/k ,$$

where k is the coefficient of thermal conductivity and c is the heat capacity per unit volume of the material.

An argument in the kinetic theory of gases leads to the following expression for the thermal conductivity:

$$k = (1/3)cv\bar{\lambda} ,$$

where v is the average particle velocity and $\bar{\lambda}$ is the mean free path.

In the case of a solid, there are excitations in the crystal lattices and insofar as they are mobile these excitations give rise to heat conduction. An argument analogous to that of the kinetic theory of gases can be given to express the thermal conductivity by an expression

similar to the preceding one:

$$k = (1/3) \sum c_a v_a \bar{\lambda}_a ,$$

where the index a denotes the kind of excitation and the summation is over all of the excitations involved in the transport of energy. There are two principle kinds of excitations of primary concern here: lattice vibrations (phonons) and free electrons. Therefore the thermal conductivity will be composed mainly of two parts, one part due to phonon and one part due to electronic contribution.

For pure bismuth at low temperatures one would expect the contribution of the electron gas to the thermal conductivity to be negligible in comparison to the phonon contribution (10). For the carbon samples employed the electronic contribution to the thermal conductivity at low temperatures could in principle be calculated if the type and the concentration of the impurities was known. Since this information is lacking, making the assumption that the concentration of possible impurities in the carbon was not too high, the dominant heat carriers at low temperatures are phonons as well. It can then be stated that the thermal conductivity of both bismuth and carbon is given by:

$$k = (1/3) c_{ph} v_{ph} \bar{\lambda}_{ph} ,$$

from which:

$$(c/k)_{ph} = (3v_{ph} \bar{\lambda}_{ph})^{-1} ,$$

where $\bar{\lambda}_{ph}$ is the phonon mean free path and v_{ph} denotes the average group velocity of phonons. Therefore the temperature relaxation time for bismuth and carbon is inversely

proportional to the corresponding mean free path:

$$\tau \sim (v_{ph} \bar{\lambda}_{ph})^{-1} .$$

The mean free path of phonons in bismuth is probably much larger than the mean free path of phonons in carbon. Under this assumption it is seen from the above formula that the temperature relaxation time of bismuth is much less than for the carbon. This argument shows that it is reasonable to expect that the carbon resistor might not respond to an existing surface temperature overshoot.

There is still more evidence that the overshoot exists. It has been suggested (11) that the temperature overshoot can be understood as a result of the behavior of the helium bath. The whole argument is based on a simple thermodynamic idea and takes into account a property concerning the mass density of the liquid helium. According to this argument, when a solid is immersed in the helium bath, the Van der Waals interactions between the helium molecules and the surface of the solid cause the density of liquid helium within a microscopic layer right next to the surface to be higher, than in the bulk of the liquid. This is expected to be true not only for helium but for any other noble liquids too. (12). The density distribution is represented in Fig. 25.

Considering a system at equilibrium, consisting of a small cube of liquid helium right next to the surface, let P , V , T denote its state variables. Due to the higher density of the system, initially its state on a TV diagram

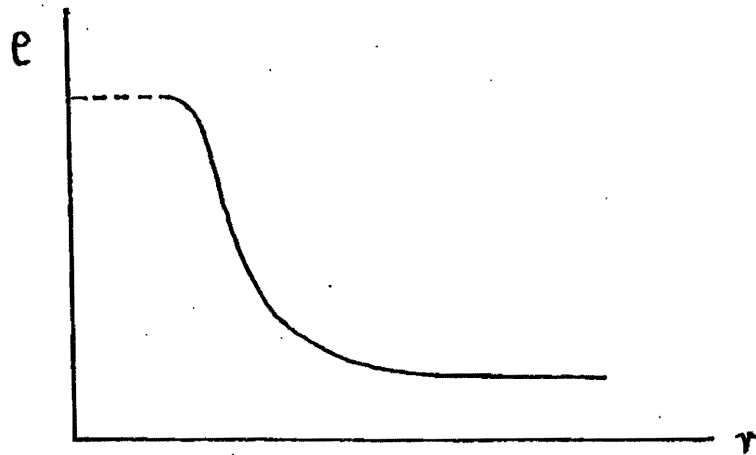


Fig. 25. Density of liquid helium as a function of the distance r from an immersed surface.

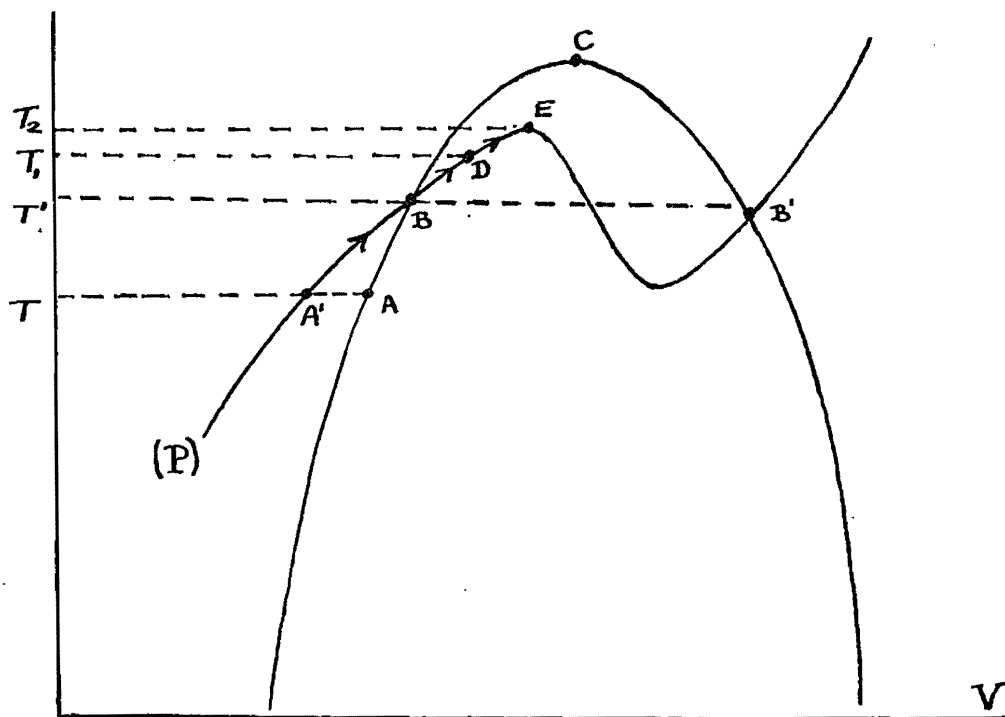


Fig. 26. Diagram for a possible explanation of the overshoot.

is not represented by a point A lying on the liquid saturation curve but by a point A' in the liquid phase (Fig. 26).

When a current is passed through the solid, then the temperature of the surface is increased and consequently the system undergoes a transition along a generally complicated path, but let it be supposed the transition is isobaric. Starting from point A' the system "moves" along the isobar (P) and arrives on the liquid saturation curve at point B. After reaching point B the system does not necessarily move along the path BB', but if there are not many impurities to trigger a phase transition, may continue "moving" on the path BE, being in a metastable state. For moderate heating of the surface i.e. relatively small currents, the system cannot reach point E, but when it has reached an intermediate point D, something starts the phase transition (it is believed that bubbling begins here) and the system relaxes back to the temperature T'. If however, the applied electrical power is high enough the system "moves" more rapidly toward point E, after which it immediately relaxes back to temperature T'.

The surface of the solid follows the temperature variations of the helium. According to Fig. 26, for moderate power inputs, the surface temperature of the solid starts from T, increases up to a maximum temperature T₁ and falls back to the steady state value T'. This accounts for temperature overshoot, ΔT at the overshoot being:

$$\Delta T = T_1 - T \quad .$$

For high power inputs the surface temperature of the solid increases rapidly up to T_2 and immediately falls back to the steady state value T' . This accounts for the sharp break, ΔT at the break, being equal to:

$$(\Delta T)_{\text{break}} = T_2 - T \quad .$$

The same argument holds without being necessary to assume the dense liquid helium layer next to the heated surface. In such a case though, the system starts from a point lying on the bulk helium coexistence curve and therefore the predicted ΔT 's will be less because less energy is needed to cause a phase transition.

CONCLUSIONS AND RECOMMENDATIONS

The earlier observations of the temperature overshoot using bismuth crystals have been verified, but the attempts to reproduce those results by using carbon have been unsuccessful. It is believed though, that such a peak really exists, and it seems that it is connected with the heat transfer across the carbon-liquid helium I interface.

From the experimental point of view a method of constructing a carbon sample delicate enough to satisfy all the requirements should first be developed. The idea of carbon film samples is the most attractive. It is known that carbon films are widely used in low temperature thermometry (13), but in all cases their resistance turns out to be too high for the experimental set up. So modifications are necessary in order to overcome the problem of their high resistance at liquid helium temperatures. However if improvement of the carbon film samples is impossible then it would be worthwhile to change the experimental equipment. For example, an apparatus similar to the one used by Smith and Giventer (2), where the resistance measurements were taken by the bridge method, might be convenient.

Furthermore it would be advantageous to extend the experiment to cover a larger range of semimetals and semiconductors. Semi-metallic antimony or arsenic and semiconducting germanium or silicon might be our next best

choice. However with semimetals we face the problem of growing single crystals, while with semiconductors the problem lies in their low conductivity coefficient. Since the melting point of both antimony and arsenic is higher than the melting point of pyrex used for the growth of bismuth single crystals, a different material must be used in the procedure of growing antimony and arsenic single crystals. As far as the low conductivity of semiconductors is concerned, thin germanium or silicon crystals highly doped might be used.

From a theoretical point of view, the nucleate boiling mechanism should be reconsidered. It seems that nucleate boiling by itself, without the introduction of some extra parameter, does not account for the observed peak of ΔT . One or more parameters should be introduced in addition to nucleate boiling in such a way that the theoretical calculation of ΔT predicts the overshoot in the transient region.

Such a parameter was introduced by Takeo (14). He considered a model according to which there is a delay time for the activation of the nuclei. With this assumption the heat transfer problem for the transient state led to a complicated differential equation for ΔT as a function of time, the solution of which was obtained by numerical methods. A plot of computer data showed a slight temperature overshoot. Of course this is not complete but it at least gives some support for the existence of an overshoot.

A different mathematical model based on the same basic

nucleation mechanism should be developed to clearly predict the overshoot and the sharp break observed in the case of bismuth. After the nucleate boiling idea has been adopted to account for these effects a study could be carried out to check these ideas experimentally. Smoothing or roughing the surface of the crystal should have drastic effects on the population of active nuclei available for nucleate boiling. Accordingly the peak effect should be more or less pronounced, depending upon the surface condition.

With negative results at the moment no further conclusions can be drawn concerning the nature and reproducibility of the earlier mentioned experimental results with bismuth. It is hoped though that the present work will be the starting point of a new series of experimental as well as theoretical attempts for further investigation. We expect that a systematic research on this subject will produce results and ideas which will improve our rather incomplete understanding of the phenomena.

LIST OF REFERENCES

1. Luce, L. D., M.A., thesis unpublished
2. L. L. Giventer and J. L. Smith, Transient Pool Boiling of Liquid Nitrogen Due to a Square-Wave Heat Flux
Adv. in Cryogenic Engineering 15, 259-270 (1970)
3. D. N. Lyon, Boiling Heat Transfer and Peak Nucleate Boiling Fluxes in Saturated Liquid Helium between the Lambda and Critical Temperatures
Int. Adv. in Cryogenic Engineering 10, 371-379 (1965)
4. R. D. Cummings and J. L. Smith, Boiling Heat Transfer to Liquid Helium
Bull. Int. Inst. Ref. Annex, 85-95 (1966)
5. J. W. Westwater, Boiling Heat Transfer
American Scientist 47, 427 (1959)
6. M. D. Reeber, Heat Transfer to Boiling Helium
Journal of Applied Physics 34, 481-483 (1963)
7. G. K. White, Experimental Techniques in Low Temperature Physics, Oxford
8. J. R. Clement and E. H. Quinnell,
Rev. Scient. Instrum. 23, 213 (1952)
9. Seki and Ames, Effective Thermal Conductance From a Thin Film into Liquid Helium
J. Applied Physics 35, 2069 (1964)
10. Ziman, Electrons and Phonons, Oxford
11. J. S. Semura and J. Opsal, Private Communication
12. Challis, Dransfeld and Wilks, Heat Transfer Between Solids and Liquid Helium II
Proc. Roy. Soc. (London) A260, 31 (1961)
- Sabinsky and Anderson, Verification of the Van-der Waals Potential Using Liquid Helium Films
Phys. Rev. A7, 790 (1973)
13. W. F. Giauque, J. W. Stout and C. W. Clark,
J. Amer. Chem. Soc. 60, 1053 (1938)
14. M. Takeo, Private Communication